IOP Conf. Series: Materials Science and Engineering **730** (2020) 012013 doi:10.1088/1757-899X/730/1/012013

Analysis of T23 Steel Weld-Joint on the Stress Relaxation Crack at Medium Temperature

Zhiqiang Sun[1], Yuwei Wang[2], Zhongbing Chen[1], Yu Zhang[2], Yongsan Ding[2], Hongbin Zhu[2] and Shaohua Yin[1]

1.Suzhou Nuclear Power Institution,1788 XIhuan Road, Suzhou, P.R. China
2.China Energy Jiangsu Power Co., Ltd.,Jianbi Power Plant, Jianbi Town, Zhenjiang City, P.R.China
E-Mail:13776254398@163.com, 12065569@chnenergy.com.cn, czbing2000@163.com, zy839783@163.com, yongsan.ding@chenergy.com.cn, zhulv2012@163.com, yinshaohua@cgnpc.com.cn

Abstract. This paper issues a new type of reheat-crack of T23 steel weld which is deferent to the cracks occurred at higher temperature above 550 degree as literatures reported. The specimen to be studied taken from a unit with long service time is analyzed by means of metallographic, scanning electron microscopy and energy dispersive spectroscopy. When further in-depth analysis is carried out on the test results, we find that Ti (Al) -N compounds are precipitated at grain boundaries, promote the formation of cavities, and finally become crack. Although the temperature of the crack is only about 380 degree which is much lower than the reheat-crack sensitivite temperature limit of T23 steel, but we also regard this crack as a type of stress relaxation crack which is another form of reheat-crack in coarse grained region of T23 steel weld-joint under specific service environment.

1. Introduction

HCM2S steel, which is a kind of bainite heat-resistant stee researched and developed by Sumitomo Corporation of Japan, has been used of high temperature components such as water-wall of high parameter thermal power plants in China in recent years. This steel is developed on the basis of T22 steel with the characterise of adding tungsten (W) ,which partly replacing molybdenum(Mo), niobium(Nb) and vanadium(V) , and reducing the carbon content to 0.04%~0.10% at the same time. The ASME grade of this steel is ASTM213-T23. The chemical composition and the mechanical properties at room temperature of T23 steel are respectively indicated in table 1 and 2(Ref.1). Comparated the allowable stresses at 540~580 degree temperature of the steels of HCM2S, 12Cr1MoV and T22, the value of HCM2S is 1.3 times as much as that of 12Cr1MoV and 1.8 times as much as that of T22(Ref.2). Therefore, as a result of the high allowable stress at elevated temperatures, the use of T23 steel in water-wall can effectively reduce the tube thickness and then improve the heat transfer rate. At the same time, T23 steel has a low carbon content, which can improve the weldability and is convenient for water-wall installation (Ref.3~4).

In recent years, many failure cases of T23 water wall tube butt-joints have been reported in China(Ref.5~7). But few literatures have been published on the analysis of T23 steel water-wall fin welds. Because water-wall is the largest and most complex component in power plant, the butt-joints and the fin welds are both the key weld joint structure. So, it is necessary to analyze the performance

of the fin weld of T23 steel water-wall undergoing long service time of 1000MW ultra supercritical unit. This paper does it, and aims to provide relevant experience for similar units.

Table 1. Chemical composition of T23 steel (Wt,%)

Elements	*C*	*Mn*	*P*	*S*	Si	Cr	Mo	V	Ti	W	Nb	N	Al
min.	0.04	0.10	-	-	-	1.9	0.05	0.20	n.s.	1.45	0.02	-	-
max.	0.10	0.60	0.03	0.01	0.50	2.6	0.30	0.30		1.75	0.08	0.03	0.03

Note: n.s. in this table indicates that there is no redulation.

Table 2. Mechanical properties of T23 steel

Yield strength(MPa)	Tensile strength(MPa)	Elongation(%)	Maximum hardness(HB)
≥400	≥510	≥20	220

2. Experimental Materials

The experimental materials are taken from the vertical section of water-wall of a 1000MW ultra supercritical unit which has been put into service from 2013. The materials of tube and fin are T23 steel with the tube specification of OD38.1×THK6.8(mm), and T12 steel with the 6mm thickness. The tube and fin are welded together by R307 electrode. During the maintenance period in 2019, many incomplete penetrated fin welds at the root which were welded during installation period are observed, as shown in Fig.1. We pick up sample of the this kind of weld-joint to analyse.

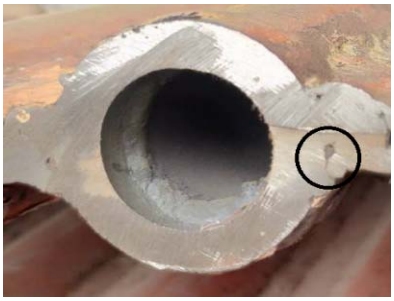

Figure 1. Incomplete penetration fin weld

3. Analysis of the Crack Characterises

3.1. Macroscopic and Microscopic Characteristics Analysis

It is observed by visual that a crack propagates from the root of the fin weld towards the inner wall of the tube after the specimen is polished and corroded by 4%H3NO3 alcohol solution, as shown in Fig.2. The same crack is also observed in another specimen with the same weld-joint structure, as shown in Fig.3.

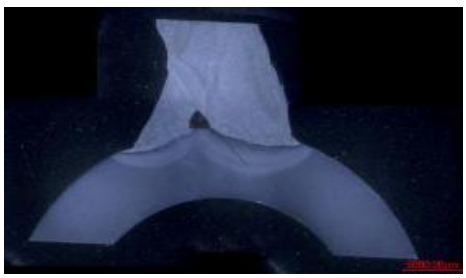

Figure 2. The crack 1 appearance of fin weld

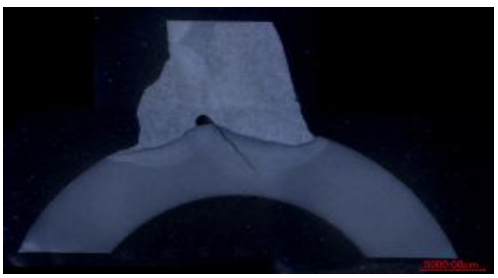

Figure 3. The crack 2 appearance of fin weld

The following characteristics of cracks are observed under the inverted universal metallographic microscope of ZEISS AXIOVERT 200 MAT.

At the starting stage, the crack initiates and extends parallel to the fusion line in the coarse grain region, and then extends towards the inner wall of the tube, finally ends in the fine grain region, as showed in Fig.4.

There are many defects are observed nearby the main crack, such as cavities, secondary cracks and so on. It is also found grey oxides in both the main crack and the secondary crack, as showed in Fig.5, 6 and7.

The crack ends are blunt, and small defects such as dense cavities are found around the ends. The cracks are also filled with gray oxide, as showing in Fig.8.

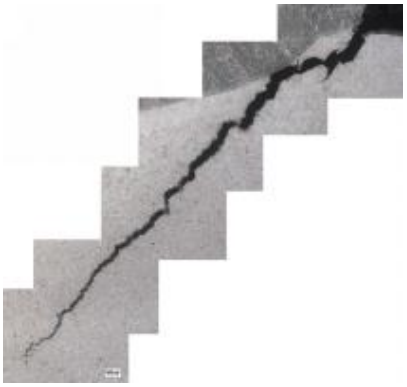

Figure 4. Appearance of the crack

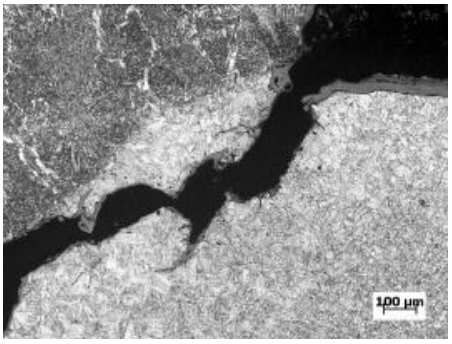

Figure 5. Appearance of the crack-start

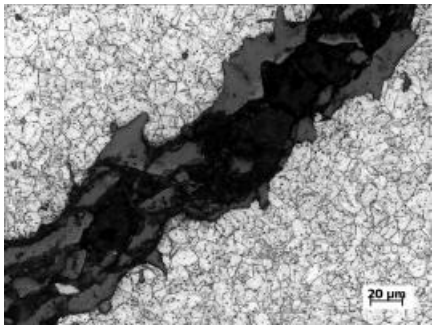

Figure 6. Appearance of the crack propagation in CGHAZ

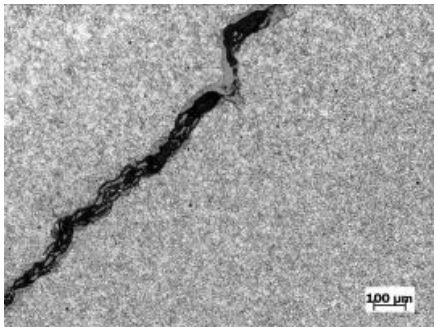

Figure 7. Appearance of the crack propagation in FGHAZ

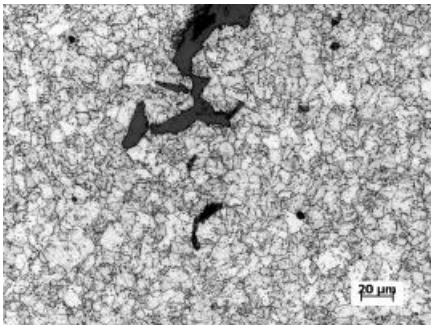

Figure 8. Appearance of the crack end

Scanning electron microscopy is used for further observation. Three kinds of defects were found around the main crack (MC), namely branching crack (CB), accompanying crack (CC) and cavity (H),

see Fig.9 and 10. The crack branching (CB) and accompanying crack (CC) are all secondary cracks.

Fig. 9 displays the blunt ends of CB and CC, and the cavities morphology at the end of CB. Both the cracks are filled with gray oxide. The results of EDS displays that the grey oxide is high temperature oxide of Fe, such as Fe3O4, as showed in Fig. 10. The phenomenon indicates that the cracks are oxidized at high temperature for a long time after they are developed.

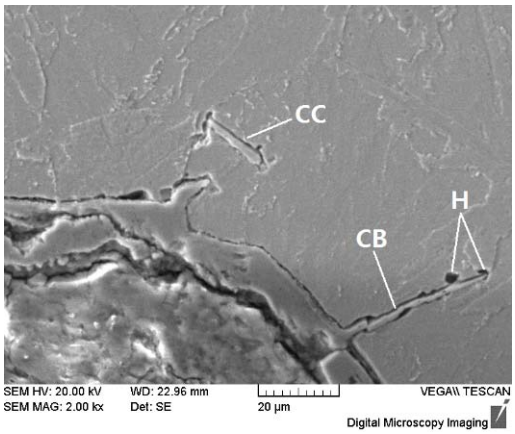

Figure 9. Appearance of secondary crack nearby the main crack

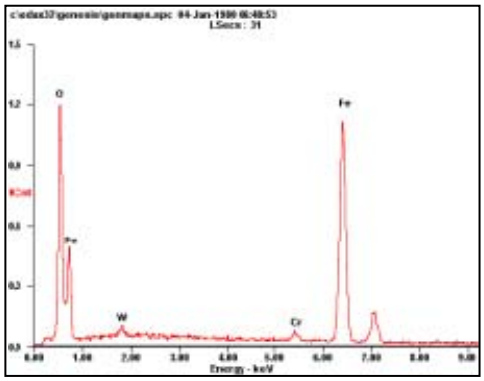

Element	*Wt%*	*At%*
OK	24.04	53.14
WM	02.99	00.57
CrK	01.66	01.13
FeK	71.32	45.16
Matrix	Correction	ZAF

Figure 10. EDS results of oxide in the secondary crack

Fig.11 reveals the appearance of two concomitant cracks (CC1,CC2) and several cavities(H1-H4) around the main crack. The concave and convex edges of CC1 show that the micro-cracks are formed after the connection of multiple cavities. But there is no grey oxide found on the surface of CC1. This is because CC1 is a newly formed crack and has not yet been oxidized. The CC2 crack has relatively straight edges, and is filled with oxide. Its characteristics are as same as those in Fig.9. The precipitates can be seen at the center of the H1-H4 cavities which grow at the triple junction of grain boundaries. EDS results of the precipitates of H4 show that it is a Ti (Al) - N compound, see Fig.12.

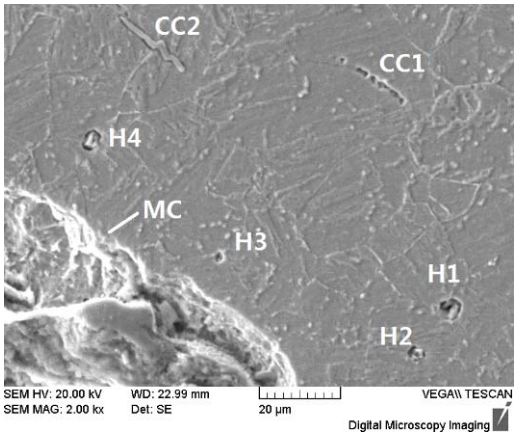

Figure 11. Appearance of concomitant cracks and cavities

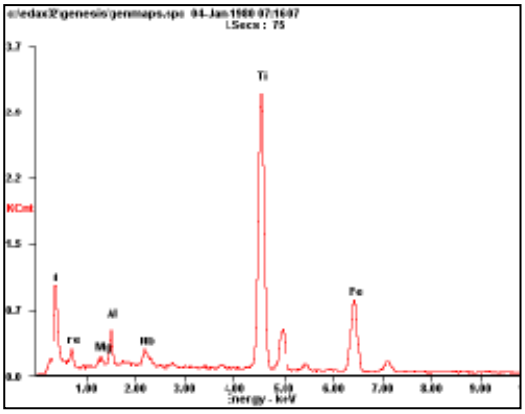

Element	*Wt%*	*At%*
NK	23.88	51.97
MgK	00.97	01.21
AlK	03.95	04.47
NbL	02.65	00.87
TiK	44.95	28.61
FeK	23.60	12.88
Matrix	Correction	ZAF

Figure 12. EDS results of the precipitate in the hole of H4

Fig.13 shows the appearance of the metal precipitate a, cavity b which is left after the precipitate shedding, and microcrack c which is formed by the cavities connection. EDS results of the precipitates c show that both the precipitate in Fig.14 and those in Fig. 11 are all Ti (Al) -N compounds.

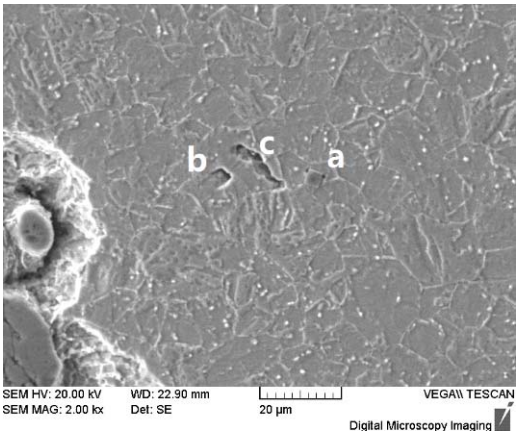

Figure 13. Appearance of the metal precipitates, voids and microcrack

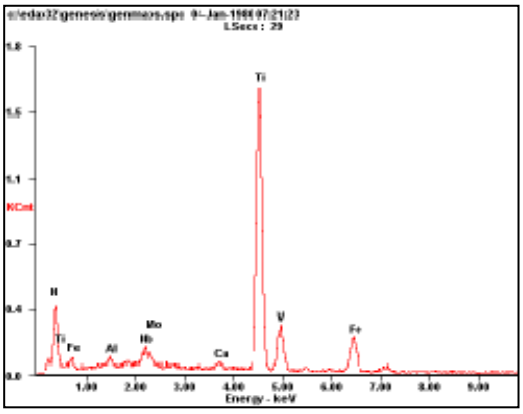

Element	Wt%	At%
NK	19.96	47.32
AlK	00.96	01.18
NbL	04.08	01.46
MoL	01.60	00.55
CaK	00.78	00.65
TiK	57.09	39.57
VK	00.67	00.44
FeK	14.84	08.82
Matrix	Correction	ZAF

Figure 14. EDS results of the metal precipitate

Fig. 15 and 17 are two wedge cracks found near the main crack. The EDS results show the elements of Ti, Al, N and O are all exist in both the cracks. Comparing the proportion of Ti and O between the two cracks(Fig.16,Fig.18) and H4 cavity(Fig.12), it is found that the proportion of Ti in the two cracks is significantly lower than that in H4 cavity. Accompany with the expansion of the wedge crack, the proportion of Ti decreases from 17.27%(Fig.16) to 9.08%(Fig.18), while the proportion of O increases from 8.06%(Fig.16) to 33.20%(Fig.18) at the same time. This indicates the process of the wedge crack that the cavities are firstly formed around the metal precipitates of Ti and other metal elements, and then partially oxidized.

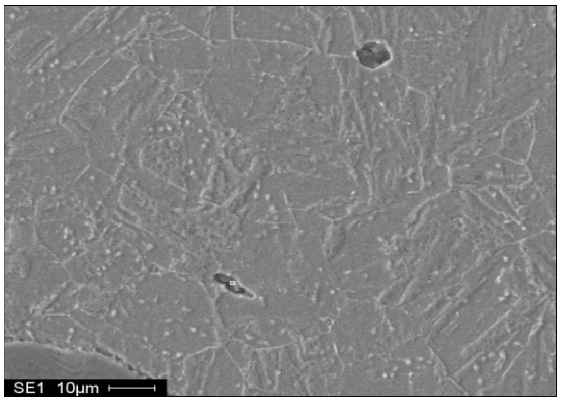

Figure 15. Wedge crack 1 near the main crack

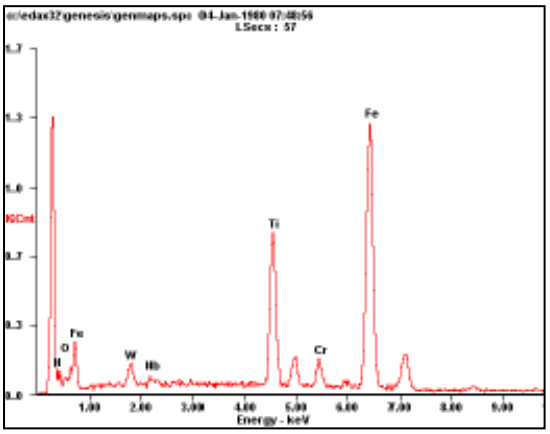

Element	Wt%	At%
NK	04.77	15.79
OK	02.78	08.06
WM	05.04	01.27
NbL	00.99	00.49
TiK	17.86	17.27
CrK	04.07	03.63
FeK	64.49	53.49
Matrix	Correction	ZAF

Figure 16. EDS results of the wedge crack1

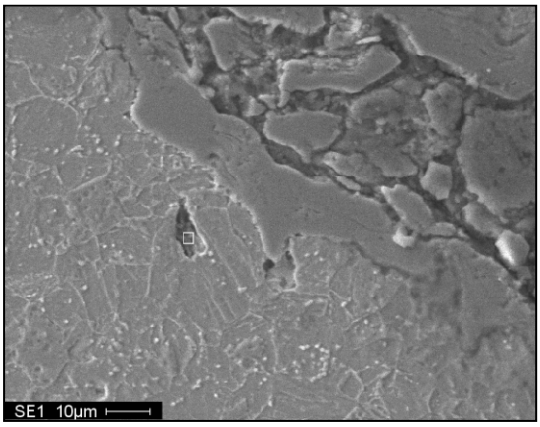

Figure 17. Wedge crack 2 near the main crack

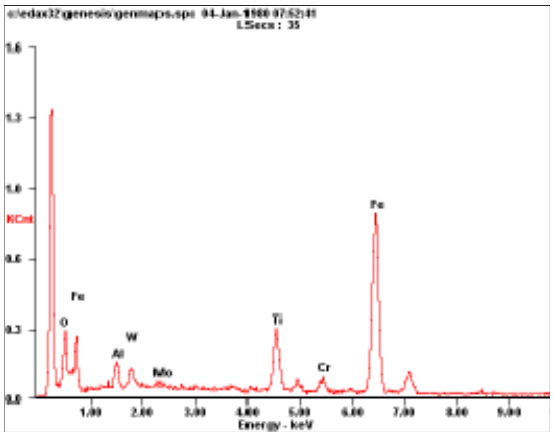

Element	Wt%	At%
OK	12.45	33.20
AlK	03.32	05.25
WM	07.22	01.68
MoL	01.35	00.60
TiK	10.19	09.08
CrK	03.23	02.65
FeK	62.24	47.55
Matrix	Correction	ZAF

Figure 18. EDS results of the wedge crack2

Fig. 19 shows the appearance of dense cavities a, wedge crack b, micro-crack c with the boundary oxidized and completely oxidized crack d. The crack end is blunt, and the crack interior is filled with gray oxide. The cavities have the exact same characteristics as those in Fig.11. The EDS results are also similar to those of both Fig.12 and Fig.21. The EDS results of the wedge crack b show that element Ti isn't found, but the proportion of O is so high to 33.97%, as showed in Fig. 22, that is probably due to the oxidation and shedding of the crack.

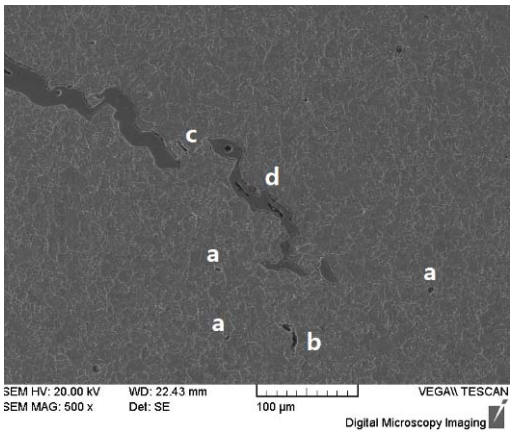

Figure 19. The whole appearance of the crak end

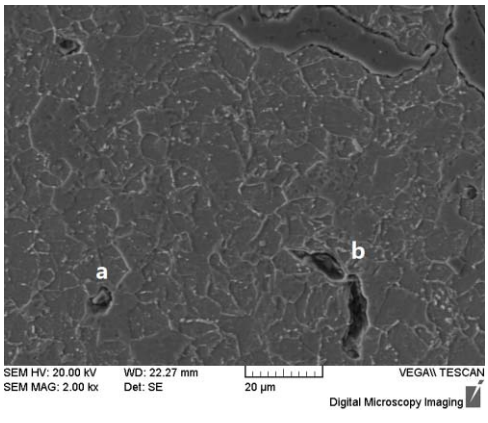

Figure 20. Appearance of the cavities and micro-crack in the crack-end

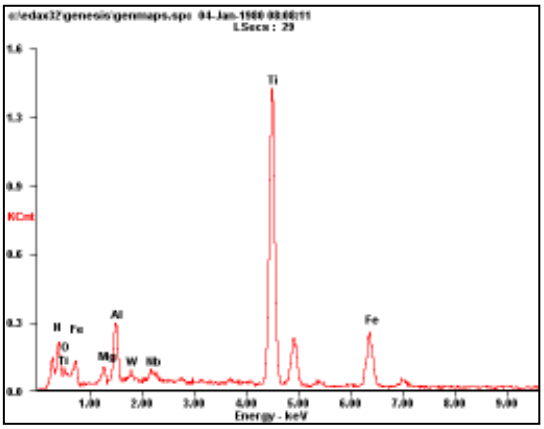

Element	Wt%	At%
NK	10.81	25.63
OK	08.43	17.50
MgK	02.15	02.93
AlK	06.21	07.64
WM	02.54	00.46
NbL	02.13	00.76
TiK	48.75	33.79
FeK	18.96	11.27
Matrix	Correction	ZAF

Figure 21. EDS results of the precipitate in the cavity

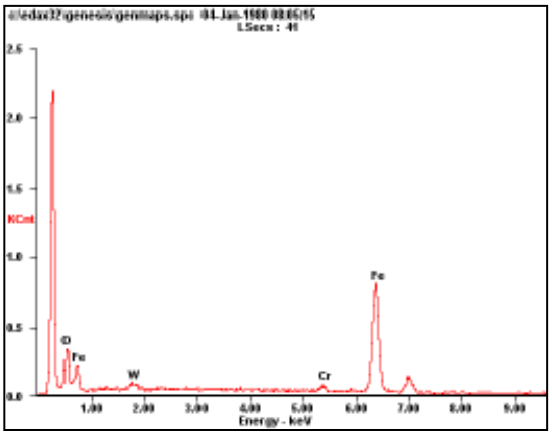

Element	Wt%	At%
OK	12.35	33.97
WM	05.76	01.38
CrK	02.54	02.15
FeK	79.34	62.50
Matrix	Correction	ZAF

Figure 22. EDS results of the wedge crack

3.2. Summary of Crack Characteristics

1)Cracks initiate in the *CGHAZ* of weld-joints. Firstly, they propagate along the fusion line in the CGHAZ, then extend towards the inner wall of the tube, finally end in the FGHAZ.

2)Many secondary cracks, such as branch cracks(CB) and accompanying cracks(CC), are found in the zone near the main crack. The main cracks and secondary cracks have blunt tips, and is filled with gray oxide, probably as Fe3O4.

3)The cavities around the crack germinate and grow at the core of metal precipitates, as Ti(Al)-N.

4)There is an inevitable relationship between the crack and the cavities from the evidence of Ti(Al)-N precipitates found both in wedge crack and cavities. The oxidation is the same step of the cracks growing, and the macrocraks are finally formed from many wedge cracks.

4. Analysis and Discuss

Based on the reheat crack theory, the crack is made as following. Firstly, the material is transformed to austenite due to primary heating, which is transformed into martensite or bainite with higher hardness during cooling stage. Secondly, in the process of reheating, the strengthening elements preferentially precipitate inside the grains, which would strengthen the grains and weaken the grain boundaries. When reheating, stress relaxation causes the slide between grain boundaries, but the grains are too strong to deformation. Under the dual action of stress relaxation and precipitate strengthening (hardening), stress will be concentrated on the boundaries of gain, so the crack is occured(Ref.8-9). The typical characteristics are that the crack initiates in the coarse grain region, propagates parallel along the fusion line and ends in the fine grain region(Ref.10-11). But the crack of this paper has its own typical characteristics in the respects of generation condition, micro-characteristics, crack evolution process.

Firstly, the service temperature of the crack in this paper is much lower than the reheat-cracke sensitive temperature of T23 steel which ranges from 575 to 750 degree(Ref.12-13). A lot of researches has been carried out in this temperature range. The elevated temperature aging tests on T23 steel weld show that new precipitates are detected neither inside nor at the boundaries of the weld grain at 500 degree temperature, while a small amount of secondary precipitates have just been detected until the temperature reaches to 550 degree(Ref.14). Reference 15 calculated the service temperature and stress diagram of water-wall of 1000MW unit. The results showed that the temperature of fin weld root(where cracks occur) was estimated to 380 degree, while the water wall tube was at 413.7 degree service temperature(Ref.15). This result is corresponding with reality according to the actual operating conditions of the unit. So, the temperature at which cracks occur is lower than not only the reheat-crack sensitive lower limit temperature, but also the lower secondary precipitation phase limit temperature. The Vickers hardness test on the heat affected zone shows that the average hardness reaches HV306, see the results of 7-11 number points in Fig.23. The hardness of T23 weld without high tempering heat treatment can reach HV300~350(Ref.16-18). Contrusting the two hardness values, we could draw a conclusion that the weld of this paper is not gone through high tempering heat treatment. So, the oxides filled in crack is gradually generated during long-term exposure in high temperature environment.

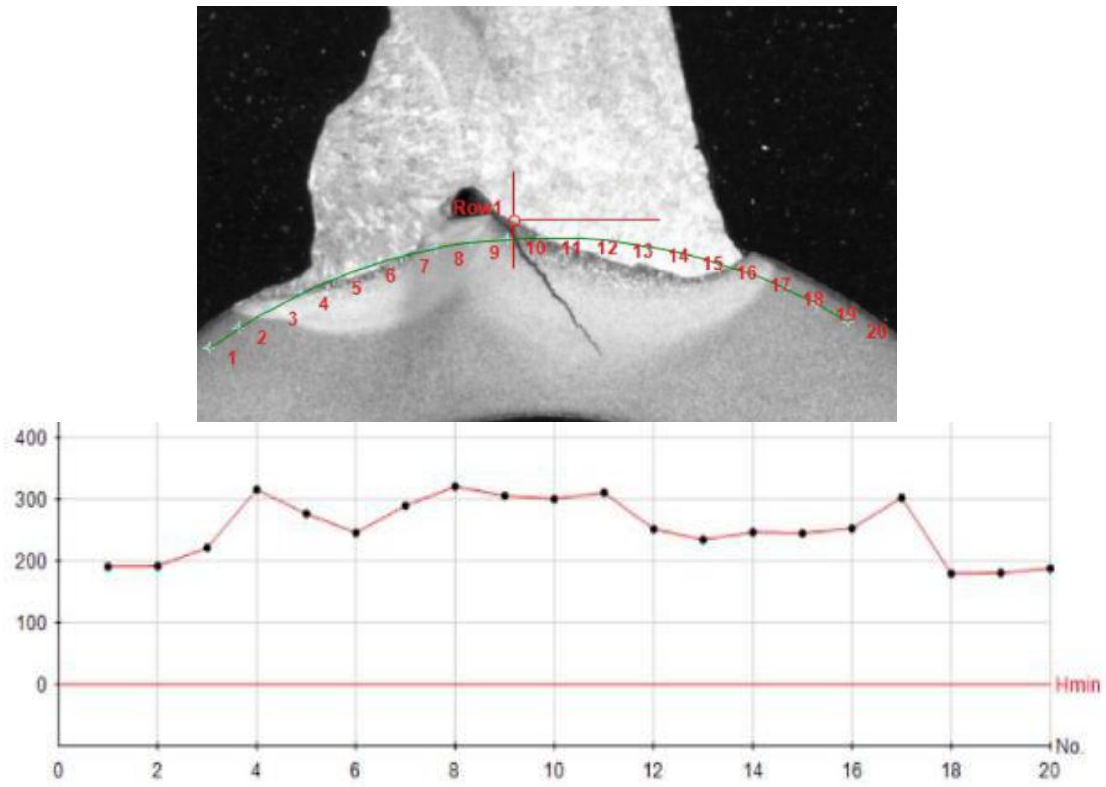

Figure 23. Hardness results of weld-joint HAZ

Secondly, according to the above analysis, it is not hard to evolute the process of cracks. In the first period, the cavities are bred with metal inclusion as the core. Then, the wedge cracks are developed at the grain boundary, especially at the trigeminal grain boundary. After a serial procedure of oxidation, propagation and connection of microcracks, the macro-cracks are finally formatted. The metal inclusion refer to Ti(Al)-N which is separated out during welding. The TiN inclusion near the trigeminal grain boundary will significantly reduce the grain boundary strength as the cause of cavities initiated by TiN, as reported in reference 19(Ref.19). The TiN appearance in this paper is exactly the same as that in reference 19, as showed in Fig.24 and Fig.13. Aluminum is ofen used as deoxidant metal during steel-making. It is also repeorted that AlN can largely reduce the creep properties of T91

steel as the core of creep cavities at grain boundaries(Ref.20). So, we can conclude that the Ti(Al)-N inclusion can cause the cavities, decrease the bonding strength at grain boundaries, and promote the formation of cracks in this paper.

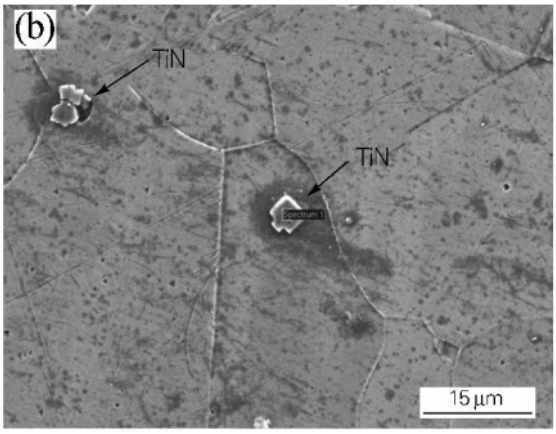

Figure 24. Morphology of TiN Compounds in Reference Document 19(Ref.19)

Finally, there are two main factors on the generation of reheat-cracks in T23. One is the material grain has so high strength that it is hard to make deformation inter grain. During stress relaxation, stress are concentrated on the grain boundaries. The other is the precipitated phases and inclusions at grain boundaries which play a pinning role to hinder the sliding between grain boundaries and cause stress concentration. In this paper, the coarse grain zone has high hardness, and the Ti(Al)-N inclusion is found at the grain boundaries at the same time. So, the two factors of reheat-crack are met. Reference 21 reports two failure modes, which are intergranular failure (IG) and plastic tearing (DT) after high temperature stress relaxation simulation test on the coarse grain zone of T23 steel weld. With the increase of temperature, the amount of Fe-rich M3C phases increases at grain boundaries, and the IG ratio relevantly increases from 40% to 60% at 575 degree to 80% to 100% at 725 degree(Ref.21). So, it is conducted that the main failure mode of crack in this paper is mainly of plastic tearing(DT) for the reason that the service temperature is much lower than 575 degree. Because the plastic tearing(DT) has much lower growthing speed than intergranular failure (IG), the crack has enough time to be oxided. It is proved by the crack blunt shape tip which is the evidence of continue oxiding.

Based on the above discussion results, the author considers that the crack in this paper is a kind of stress relaxation crack in welded joints of T23 steel, and it is also another form of reheat crack in medium temperature environment.

5. Conclusion

1)The cracks of the fin weld initiate in the coarse grain zone of the heat-affected zone, extending parallel to the fusion line at first, then developing towards the inner wall of the tube, ending at the fine grain zone at last. After a thorough study on the microcosmic characteristics and inclusion, it is concluded that the crack is stress relaxation crack caused by metal inclusion, and is another form of reheat crack of T23 steel weld-joint in medium temperature environment.

2) The Ti(Al)-N inclusion in T23 steel weld greatly reduce the grain creep strength, generate cavities at grain boundaries, promote to form wedge cracks, and finally come into being macrocracks.

6. Reference

[1] Yang fu, Zhang yinglin, Li weimin, et al. Welding of New Type Heat-Resisting Steel[M].Beijing: China Power Press,2006:69-73.

[2] Pan qiangang. Prospective forecaste of HCM2S Steel Used in Boiler of Our Country[J].Electric Welding Machine,2004,34(05):6-11.

[3] Ji xianwu, Duan peng, Li ju, et al. Application of T23 Steel to 1000MW Ultra-supercritical Units[J].East China Electric Power, 2009, 37(12):2097-2101.
[4] Zhang eying, Wang xiangbin, Tao shengzhi, et al. Application of T23 Steel in Large-Scale Conventional Utility Boilers[J].Thermal Power Generation,2005,34(3):68-73+77.
[5] Li shengwen, Lin lin, Zhang shiming. Failure Analysis and Prevention on T23 Steel Joints of Water Wall in USC Tower Boiler[J].Foundry Technology,2017,38(9):2159-2161.
[6] Li wenbo, Shen dingjie, Xie yi, et al. Failure Analysis on Weld Joint of T23 Heat-resistant Steels[J]. Power Equipment, 2015, 29(6):443-446.
[7] Sun biao. Analysis on T23 Steel Welded Joint Failure and Welding Process Based on Ultra Supercritical Unit[J].Hot Working Technology, 2016, 45(9):250-252+258.
[8] John C. Lippold. Welding Metallurgy and Weldability[M].Beijing: China Machine Press, 2016:110-114.
[9] J.G.Nawrocji, J.N. Dupont, C.V.Robino and A.R.Marder. The Stress-relief Cracking Susceptibility of a New Ferritic Steel Part 1: Single-pass Heat Affected Zone Simulations [J].Welding Journal, 2000, 35(12):355-362.
[10] Qiao yaxia, He zhenyu, Guo jun, et al. Craking Analysis of T23 Steel Weld -Joint of Reheater in a Power Plant[C]. Papers Collection of the Eleventh Power Station Welding Symposium, Jinan, 2011.
[11] Jin yujing, Zhou wei. Characteristics of reheat Cracking in CGHAZ of Modified T23 Steel[J]. Heat Treatment of Metals, 2017, 42(11):191-197.
[12] Wang tiantian, Xu mengjia, Xu jijin, et al. Influence of Second Welding Thermal Cycle on Reheat Cracking Sensitivity of CGHAZ in T23 Steel Influence of Second Welding Thermal Cycle on Reheat Cracking Sensitivity of CGHAZ in T23 Steel[J].Materials Review, 2017, 31(12):56-59.
[13] Wang xue, Xu delu, Chen yucheng, et al. Reheat-Crack Sensitivity of T23 Steel[C].Collected Papers of the 2009 Academic Conference on Modern Welding Science and Technology, Haerbin, 2009.
[14] Wang xue, Li xiqiang, Yang chao, et al. Aging Properities of T23 Weld Joint in Water Wall of USC Boilers[J]. Journal of Chinese Society of Pwer Engineering, 2015, 35(04): 325-335.
[15] Fan jin, Jia hongxiang, Chen tingkuan, et al. Analysis on the Temperature and Thermal Sress Fields of membrane Tube of Boiler in Power Plant[J].Journal of Xian Jiao Tong University, 1997, 31(05):75-80.
[16] Li xiqiang, Wang xue, Yang chao, et al. Effects of Preheating and Post-Weld Heat Treatment on the Mechanical Properities of T23 Steel Welding[J].Electric Power, 49(2):1-5+66.
[17] Liu yongchao. Study on CGHAZ and Reheat Cracking of T23 Steel[M].Shanghai: Shanghai Jiao Tong University:2013.
[18] Wang qijiang, Zou fengming, Deng yongqing, et al. Effect of T23 Steel's Microstructural Evolution on Its Properities[J].Bao Steel Technology,2006,(3):18-22.
[19] Cheng xiaonong, Chen ming, Li dongsheng, et al. High Temperature Creep Behavior of Fe-Ni Based Alloy Cr19Ni28TiN[J].Heat Treatment of Metals,2015,40(2):48-51.
[20] Zhu lihui, Zhao qinxin, Gu haicheng, et al. Effect of Aluminum on Creep Rupture Property of T91 Heat-resistant Steel[J].Iron and Steel, 2002, 37(5):50-54.
[21] C.V.Robino, A.R.Marder, J.D.Puskar, et al. The Mechanism of Stress-Relief Cracking in a Ferritic Alloy Steel[J].Welding Journal, 2003, 82(2): 25-S-35-S.